

Inversions and Fractal Patterns in Alpha Plane

Özcan Gelişgen* and Temel Ermiş

(Dedicated to the memory of Prof. Dr. Krishan Lal DUGGAL (1929 - 2022))

ABSTRACT

In this paper, we introduce the α -circle inversion by using α -distance function instead of Euclidean distance in definition of classical inversion. We give some properties of α -circle inversion. Also this new transformation is applied to well known fractals. Then new fractal patterns are obtained. Moreover we generalize the method called circle inversion fractal by means of the α -circle inversion. In alpha plane, \mathbb{R}_α^2 , we give a generalization of α -circle inversion fractal by using the concept of star-shaped set inversion which is a generalization of circle inversion fractal.

Keywords: Alpha circle inversion; Alpha distance; Limit set; Fractal; Star-shaped set; Star-shaped set inversion

AMS Subject Classification (2020): Primary: 28A80 ; Secondary: 51F05; 51F99.

1. Introduction

Imagine that you and your friend are in Himalayas for climbing experience. During the climb you notice something on the opposite hill, and you ask your friend: "What is the distance between here and the opposite hill?" Perhaps, you get the answer "it's about 300 meters". The answer formally correct and still absolutely useless. Of course, every mountaineers know that distance in mountains is a tricky thing. This answer may be suitable for a bird. But creatures without wings or flight equipment have to take long detours with lots of ups and downs. Similarly, if one want to measure the distance between two points on a plane, then one can use frequently Euclidean distance which is defined as the length of segment between these points. Although it is the most popular distance function, it is not practical when we measure the distance which we actually move in the real world. For every two points on a surface in Euclidean space or in the Euclidean plane we can measure Euclidean distance between the two points. What we do instead is we introduce a new distance which is measured along the shortest path between the two points. Generalizing this idea, one says that a distance function on a metric space is an intrinsic metric if the distance between two points can be realized by paths connecting the points. For example, taxicab distance and Chinese checkers distance are intrinsic metrics. Taxicab and Chinese checkers distance functions are similar to moving with a car or Chinese chess in the real world. Later, Tian [27] defined a family of metrics, α -metric (alpha metric) for $\alpha \in [0, \pi/4]$. The taxicab and Chinese checker metrics are special cases of α -metric. Then, some authors developed and studied on various aspect of these topics. For example, Gelişgen and Kaya [14, 15] extended the α -distance to three and n dimensional spaces, respectively. Afterwards, Colakoğlu [8] extended the α -metric for $\alpha \in [0, \pi/2]$. According to the latter, if $P = (x_1, y_1)$ and $Q = (x_2, y_2)$ are two points in \mathbb{R}^2 , then for each $\alpha \in [0, \pi/2]$ and $\lambda(\alpha) = \sec \alpha - \tan \alpha$, the α -distance between P and Q is

$$d_\alpha(P, Q) = \max\{|x_1 - x_2|, |y_1 - y_2|\} + \lambda(\alpha) \min\{|x_1 - x_2|, |y_1 - y_2|\}.$$

Obviously, there are infinitely many different distance function depending on values of α . But we assume that value of α are initially determined and fixed unless otherwise stated.

The linear structure of α -plane is the same as the Euclidean one. That is, the points and the lines are the same, and the angles are measured in the same way. There are only one difference. This difference is that the α -plane geometry has a different distance function. Therefore, it seems interesting to study the α -analog of the topics that include the concepts of distance in the Euclidean geometry.

One of the concepts which include notation of distance is an inversion. As stated in Kozai and Libeskind [17], this particular transformation was probably first introduced by Apollonius of Perga (225 BCE – 190 BCE). The systematic investigation of inversions began with Jakob Steiner (1796-1863) in the 1820s. During the following decades, many physicists and mathematicians such as William Thomson, August F. Möbius and Mario Pieri independently rediscovered inversions, proving the properties that were most useful for their particular applications. For more detail see Kozai and Libeskind [17], and Patterson [23].

Inversion has attracted the attention of scientist from past to present. So there are a lot of study about inversion. Many scientist studied and also are studying different aspect of this concept. In Childress [6] and Ramirez [24], the authors investigated the inversions with respect to the central conics in real Euclidean plane. The inversions with respect to taxicab circle was studied detailed in Nickel [21], and Bayar and Ekmekci [2].

One of the most famous mathematical topics in recent times is fractals. Fractal geometry is one of the rising topics of mathematics even though it is a fairly new field. The concept of fractals was first presented by Mandelbrot [20] in the 1970s. Afterwards Barnsley [1] introduced some revolutionary ideas with respect to the practical aspect of fractals. He provided methods to model natural fractals and used the concept of the iterated function system (IFS) as a tool to generate them. After that, therefore, fractal geometry has been used in many applications from pattern recognition to medicine and also even in archaeology (See [19, 5, 22] for more information).

In these application areas, fractals have been used to generate very complicated and pretty patterns. Although fractal patterns are very complex, in fact they can be generated only a small amount of information. For example, in the IFS, fractals can be produced with only information about a finite number of contractive mappings. For IFSs there are two main algorithms used to generating fractal patterns. These are deterministic algorithm and random iteration algorithm. Later in Frame and Cogeşina [9] a new method which is termed as circle inversion fractal was introduced by using circle inversion mappings. A similar method was also observed in Zhang and He [28]. This method was generalized to sphere inversions by Leys [18]. In 2007, Helt [16] used the idea inversion mapping created by using the centroids of the geometric objects instead of the idea of inversion according to the circle for 2- and 3-dimensional space, and he examined the fractals with formed by this idea. Later, Gdawiec [11] extended the method of circle inversion fractals to star-shaped sets. The Euclidean circle inversion mapping is used in all of the mentioned studies of circle inversion mappings. In 2016, Gdawiec [12] introduced new technique for obtaining new and diverse fractal patterns. According to this technique is based on the use of different metrics in the inversion mapping and a switching process between different metric spaces. In 2017, Gdawiec [13] also advanced the idea of star-shaped set inversion fractals using iterations known from fixed point theory like as Piccard, Mann Isakawa, ect. Most of the articles which some of their are listed above on this subject focuses on the graphical aspect of such fractals, without presenting a careful development of the underlying mathematical framework. In [4] Boreland and Kunze presented such a framework, making a strong connection to iterated function systems (IFS) theory. Also in [10] Fitzsimmons and Kunze showed that there exists an attractor to the iterated function system consisting of modified circle inversion maps, and that the regular chaos game generate the attractor. In 2015, Ramirez [25] et al. carried out these studies about circle inversion fractals from Euclidean plane to other plane which is furnished by Minkowski metric (p -metric) by using p -circle inversion mapping. According to p -metric, circles are oval convex closed curves except the cases of $p = 1$ and $p \rightarrow \infty$. In the cases of $p = 1$ and $p \rightarrow \infty$, the circle is a square. The Figure 1(a) presents some examples of the p -circles.

Now, in this paper we study another generalization of the circle inversion by using an α -distance. The circles in the α -plane are octagon except the cases of $\alpha = 0$ and $\alpha \rightarrow \frac{\pi}{2}$. In these excepted cases, the circle is a square as like as excepted cases of p -circle. The α -circle is generally an octagon which is not uniform. If one take $\alpha = \frac{\pi}{4}$, then the α -circle is a regular octagon. The Figure 1(b) presents some examples of the α -circles. The planes with p -metric and α -metric have similar character about circles according to changing value of p and α . The difference is that the circles in the p -plane are smooth while the circles in the α -plane are not smooth, that is, they have vertices. So we firstly introduce α -circle inversion and develop some properties of this term. Later we modify and carry out studies about circle inversion fractals to α -plane. Then new fractal patterns are obtained.

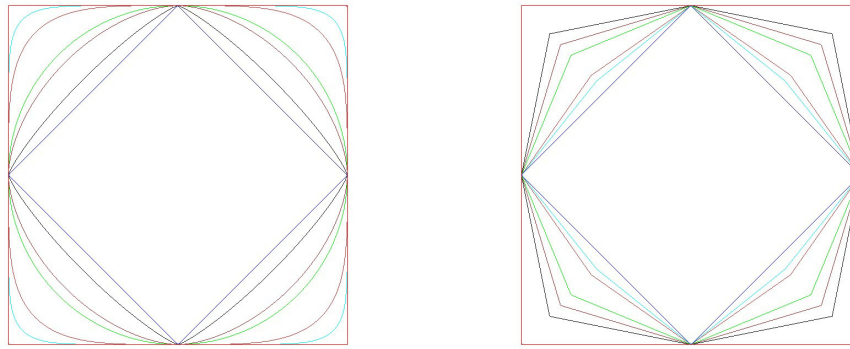


Figure 1(a): Some examples of p -circles Figure 1(b): Some examples of α -circles

2. The α -circle Inversion and Some Properties

In this section we firstly define the α -circle inversion by using the α -metric instead of the well-known Euclidean metric in classic definition of circle inversion. Later we give some properties of the α -circle inversion. Now, we give some knowledge about Euclidean circle inversion.

As it has been stated in Blair [3], in the Euclidean plane an inversion in a circle of radius r is a mapping in which a point P and its image P' are on a ray emanating from the center O of the circle such that $d(O, P)d(O, P') = r^2$. This mapping is also conformal.

Clearly if P' is the inverse of P , then P is the inverse of P' . Note also that if P is in the interior of C , P' is exterior to C , and vice versa. So the interior of C except for O is mapped to the exterior and the exterior to the interior C itself is left pointwise fixed O has no image, and no point of the plane is mapped to O . However, points close to O are mapped to points far from O and points far from O map to points close to O . Thus adjoining one "ideal point", or "point at infinity", to the Euclidean plane, we can include O in the domain and range of inversion.

Now in the alpha plane, \mathbb{R}_α^2 , the definition of inversion with respect to an α -circle can be given as follows:

Definition 2.1. Let C be an α -circle centered at a point O with radius r in \mathbb{R}_α^2 , and let P_∞ be the ideal point adjoining one to the alpha plane. In \mathbb{R}_α^2 the alpha circle inversion with respect to O is the function such that

$$I_\alpha(O, r) : \mathbb{R}_\alpha^2 \cup \{P_\infty\} \rightarrow \mathbb{R}_\alpha^2 \cup \{P_\infty\}$$

defined by $I_\alpha(O, r)(O) = P_\infty$, $I_\alpha(O, r)(P_\infty) = O$ and $I_\alpha(O, r)(P) = P'$ for $P \neq O, P_\infty$, where P' is on the ray \overrightarrow{OP} and $d_\alpha(O, P)d_\alpha(O, P') = r^2$. The point P' is called the alpha circle inverse of P according to the α -circle C , C is said to be the circle of inversion, O is called the center of inversion.

The following propositions states some basic properties which are immediately obtained from definition of the α -circle inversion.

Proposition 2.1. Let C be an alpha circle with center O and radius r and $I_\alpha(O, r)$ be an alpha circle inversion with respect to C . Then the following statements are valid.

- i) If the point P is in the interior of C then the point P' is exterior to C , and conversely.
- ii) The points of the circle C are invariant under the mappings $I_\alpha(O, r)$.
- iii) $I_\alpha(O, r)$ is involutive, that is, $(I_\alpha(O, r))^2 = \text{identity}$.
- iv) $I_\alpha(O, r)$ is a contraction on exterior of C and $I_\alpha(O, r)$ is an expansion on interior of C .

Proposition 2.2. Let $I_\alpha(O, r)$ be an alpha circle inversion with respect to an alpha circle C centered at origin and the radius r in \mathbb{R}_α^2 . If $P = (x, y)$ and $P' = (x', y')$ are inverse points according to the alpha circle inversion, then

$$x' = \frac{r^2 x}{(\max\{|x|, |y|\} + \lambda(\alpha) \min\{|x|, |y|\})^2},$$

$$y' = \frac{r^2 y}{(\max\{|x|, |y|\} + \lambda(\alpha) \min\{|x|, |y|\})^2}.$$

In more general since all translations are an isometry of \mathbb{R}_α^2 , if C is centered at the point $O = (a, b)$, then the α -inverse of point $P = (x, y)$ is stated by

$$x' = a + \frac{r^2(x - a)}{(\max\{|x - a|, |y - b|\} + \lambda(\alpha) \min\{|x - a|, |y - b|\})^2},$$

$$y' = b + \frac{r^2(y - b)}{(\max\{|x - a|, |y - b|\} + \lambda(\alpha) \min\{|x - a|, |y - b|\})^2}.$$

Proof. The α -circle C with the center at origin and the radius r consists of the points which satisfies the equation $\max\{|x|, |y|\} + \lambda(\alpha) \min\{|x|, |y|\} = r$. Let $P = (x, y)$ and $P' = (x', y')$ be inverse points with respect to C . Since the points O, P and P' are collinear and the rays \overrightarrow{OP} and $\overrightarrow{OP'}$ are same direction, $\overrightarrow{OP'} = k\overrightarrow{OP}$ for $k \in \mathbb{R}^+$. Since $d_\alpha(O, P)d_\alpha(O, P') = r^2$, it is obtained that $k = \frac{r^2}{(\max\{|x|, |y|\} + \lambda(\alpha) \min\{|x|, |y|\})^2}$. Obviously the required results are obtained by substituting the value of k in $(x', y') = (kx, ky)$. If C is centered at the point $O = (a, b)$, then one can obtain the required result by applying the translation to point $O = (a, b)$ in the previous statement. \square

The following useful properties are well known in Euclidean plane:

- i. Lines passing through the center of inversion map into themselves.
- ii. Circles with center of inversion map to circles with center of inversion.
- iii. Circles not passing through the center of inversion map into circles that do not pass through the center of inversion.
- iv. Lines not through the center of inversion map into circles through the center of inversion and conversely.

Unfortunately all of these properties which holds in the Euclidean plane are not valid in the alpha plane. The following theorem states that whether which one of these properties are satisfied or not. Since one can easily give an example for properties which do not satisfy and one can easily prove the satisfying properties by using definition of the alpha circle inversion, the next theorem is given without proof. The Figure 2 present examples for the cases of Theorem 2.1.

Theorem 2.1.

- i. The alpha circle inversion $I_\alpha(O, r)$ maps the lines passing through O onto themselves.
- ii. The alpha circle inversion $I_\alpha(O, r)$ maps the alpha circles with the center O onto the alpha circles with the center O .
- iii. The alpha circle inversion $I_\alpha(O, r)$ does not map the alpha circles not through O onto any alpha circles.
- iv. The alpha circle inversion $I_\alpha(O, r)$ does not map the lines not containing the center of the alpha circle inversion circle onto alpha circles the center O .
- v. The alpha circle inversion $I_\alpha(O, r)$ does not map the alpha circles containing the center of the inversion circle onto straight lines not containing O .

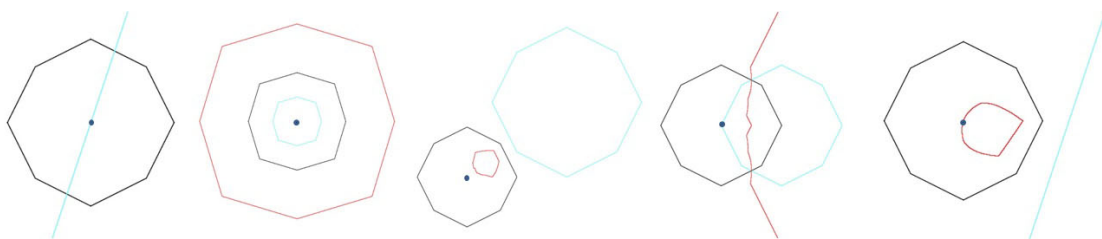


Figure 2: An example from left to right for the every cases of Theorem 2.1, respectively.

3. Some Famous Fractals and α -Circle Inversion

In this section, we will find to representations of several most familiar fractals objects under the α -circle inversion.

As stated in Smith [26], at present, there does not exist a universally agreed upon definition for ‘fractal’. Barnsley [1] defines fractal as “A fractal is a geometrically complex subset of a geometrically simple space”. Whilst this definition conveys the idea of a fractal, it is not precise in that it does not specify what is meant by ‘geometrically complex’ or ‘geometrically simple’. Thus, Barnsley’s definition is usually accompanied

by examples such as The Sierpinski Triangle, The Koch Curve and The Cantor Middle Third Set. Barnsley popularized the idea of fractal construction by means of an Iterated Function System (IFS). Now we recall the definition of IFS from Barnsley [1].

Definition 3.1. An Iterated Function System consists of a complete metric space (X, d) together with a finite set of contraction mappings $w_n : X \rightarrow X$, with respective contractivity factor s_n , for $n = 1, 2, \dots, N$. The notation for the IFS is $\{X : w_n, n = 1, 2, \dots, N\}$ and its contractivity factor is $s = \max\{s_n : n = 1, 2, \dots, N\}$. Starting with any given a non-empty compact subset of X , iteration under these maps will converge to the same set. This set, the limit set of the IFS, is termed as the attractor for the IFS.

Now we give some examples of well known fractals by generating with IFS and their representations under α -circle inversion. The each of following four example have illustrate figures. These figures are numbered as from Figure 3(a)-3(b) to Figure 6(a)-6(b). In every figure there are three objects. These are standarty the original fractal which is red one, the α inversion circle which is green one and representation of original fractal under the mapping α inversion of which is blue one.

Example 3.1. Barnsley's fern is constructed within the complete metric space $\mathbb{R}^2 \cup \{P_\infty\}$ by using following contraction mappings:

$$\begin{aligned} w_1(x, y) &= (0, 0.16y) \\ w_2(x, y) &= (0.85x + 0.04y, -0.4x + 0.85y + 0.16) \\ w_3(x, y) &= (0.2x - 0.26y, 0.23x + 0.22y + 0.16) \\ w_4(x, y) &= (-0.15x + 0.28y, 0.26x + 0.24y + 0.44). \end{aligned}$$

Barnsley's fern is the limit set of this IFS, and it is shown as red one in the Figure 3(a) and 3(b). The Figure 3(a) and 3(b) show the images (blue) of Barnsley's fern (red) under inversion with respect to the α -circle (green) for $\alpha = \frac{\pi}{4}$ and $\alpha \rightarrow \frac{\pi}{2}$, respectively.

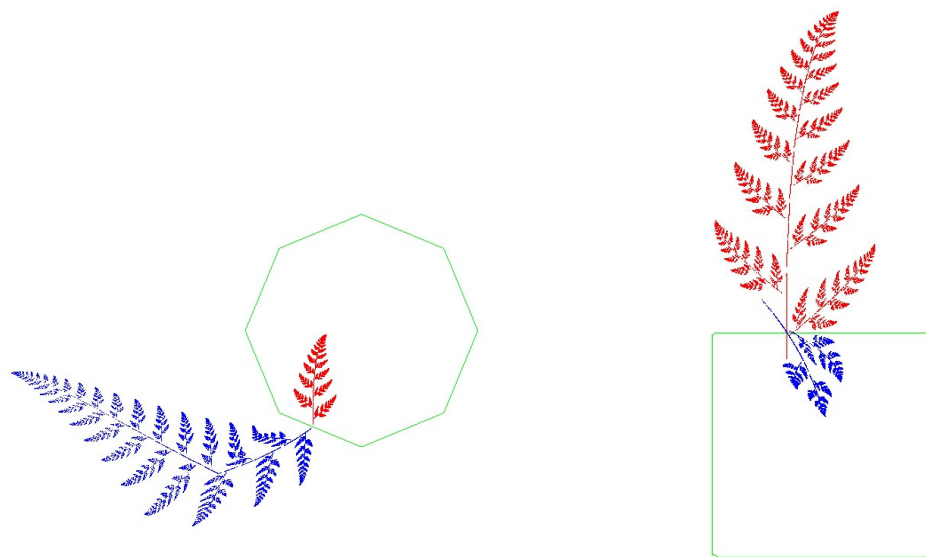


Figure 3(a)

Figure 3(b)

Barnsley's fern and its image under $I_{\frac{\pi}{4}}(O, r)$ Barnsley's fern and its image under $I_{\frac{\pi}{2}}(O, r)$

Example 3.2. The dragon curve can be obtained by using the IFS $\{w_1, w_2\}$ where

$$\begin{aligned} w_1(x, y) &= (0.5x - 0.5y, 0.5x + 0.5y), \\ w_2(x, y) &= (-0.5x - 0.5y + 1, 0.5x - 0.5y) \end{aligned}$$

and Levy dragon can be obtained by using the IFS $\{w_1, w_2\}$ where

$$\begin{aligned} w_1(x, y) &= (0.5x - 0.5y, 0.5x + 0.5y), \\ w_2(x, y) &= (0.5x + 0.5y + 0.5, -0.5x + 0.5y + 0.5). \end{aligned}$$

Figure 4 show the images of a dragon curve (left one) and Levy dragon (right one) under inversion with respect to the α -circle for $\alpha = \frac{\pi}{4}$.

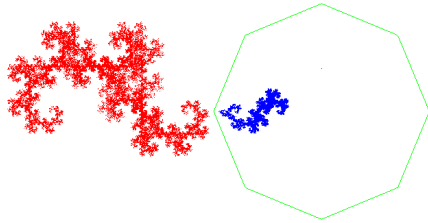


Figure 4(a)

The dragon curve and its image under $I_{\frac{\pi}{4}}(O, r)$

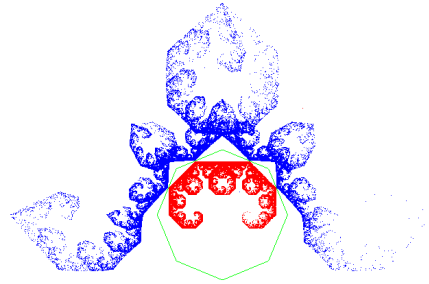


Figure 4(b)

The Levy dragon curve and its image under $I_{\frac{\pi}{4}}(O, r)$

Example 3.3. The Sierpinski triangle and Sierpinski pentagon can be obtained by using following contraction mappings:

$$\begin{aligned} w_1(x, y) &= (0.5x, 0.5y), \\ w_2(x, y) &= (0.5x + 0.5, 0.5y), \\ w_3(x, y) &= (0.5x + 0.25, 0.5y + \sqrt{3}/4) \end{aligned}$$

and

$$\begin{aligned} w_1(x, y) &= (0.382x, 0.382y), \\ w_2(x, y) &= (0.382x + 0.618, 0.382y), \\ w_3(x, y) &= (0.382x + 0.809, 0.382y + 0.588), \\ w_4(x, y) &= (0.382x + 0.309, 0.382y + 0.951), \\ w_5(x, y) &= (0.382x - 0.191, 0.382y + 0.588) \end{aligned}$$

,respectively. Figure 5 shows the images of the Sierpinski triangle (left one) and Sierpinski pentagon (right one) under inversion with respect to the α - circle for $\alpha = \frac{\pi}{4}$, respectively.

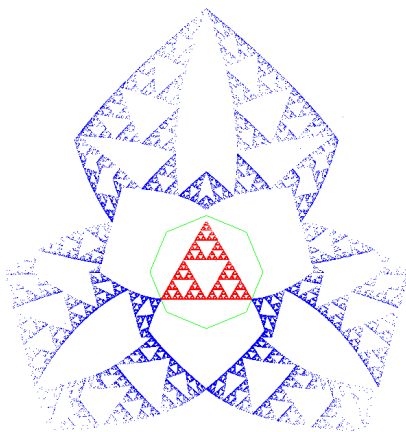


Figure 5(a)

The Sierpinski triangle and its image under $I_{\frac{\pi}{4}}(O, r)$

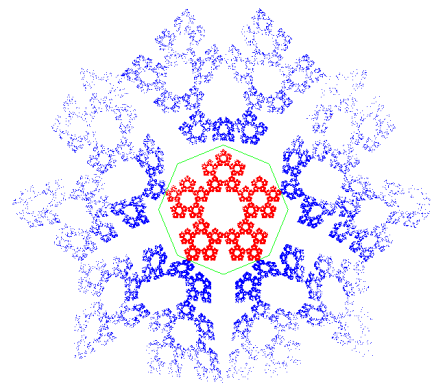


Figure 5(b)

The Sierpinski pentagon and its image under $I_{\frac{\pi}{4}}(O, r)$

Example 3.4. The Koch snowflake and the Koch anti snowflake can be generated with the following contraction mappings:

$$\begin{aligned}
 w_1(x, y) &= \left(\frac{1}{2}x - \frac{\sqrt{3}}{6}y, \frac{\sqrt{3}}{6}x + \frac{1}{2}y\right), & w_1(x, y) &= \left(\frac{1}{3}x, \frac{1}{3}y\right), \\
 w_2(x, y) &= \left(\frac{1}{3}x + \frac{1}{\sqrt{3}}, \frac{1}{3}y + \frac{1}{3}\right), & w_2(x, y) &= \left(\frac{1}{3}x + \frac{1}{3}, \frac{1}{3}y + \frac{\sqrt{3}}{3}\right), \\
 w_3(x, y) &= \left(\frac{1}{3}x, \frac{1}{3}y + \frac{2}{3}\right), & w_3(x, y) &= \left(\frac{1}{3}x + \frac{2}{3}, \frac{1}{3}y\right), \\
 w_4(x, y) &= \left(\frac{1}{3}x - \frac{1}{\sqrt{3}}, \frac{1}{3}y + \frac{1}{3}\right), & \text{and } w_4(x, y) &= \left(-\frac{1}{3}x + \frac{1}{2}, -\frac{1}{3}y + \frac{\sqrt{3}}{6}\right), \\
 w_5(x, y) &= \left(\frac{1}{3}x - \frac{1}{\sqrt{3}}, \frac{1}{3}y - \frac{1}{3}\right), & w_5(x, y) &= \left(-\frac{1}{3}x + \frac{5}{6}, -\frac{1}{3}y + \frac{\sqrt{3}}{6}\right), \\
 w_6(x, y) &= \left(\frac{1}{3}x, \frac{1}{3}y - \frac{2}{3}\right), & w_6(x, y) &= \left(-\frac{1}{3}x + \frac{2}{3}, -\frac{1}{3}y + \frac{\sqrt{3}}{3}\right), \\
 w_7(x, y) &= \left(\frac{1}{3}x + \frac{1}{\sqrt{3}}, \frac{1}{3}y - \frac{1}{3}\right)
 \end{aligned}$$

respectively. In Figure 6, one can see the images of the boundary of Koch snowflake (left one) and Koch anti snowflake (right one) under inversion with respect to the α -circle for $\alpha = \frac{\pi}{4}$. In fact the first IFS of Example 3.4 is the attractor of filled the Koch snowflake. But Figure 6(a) illustrate the boundary of it.

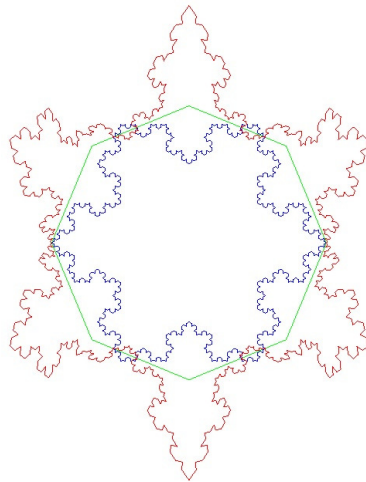


Figure 6(a)

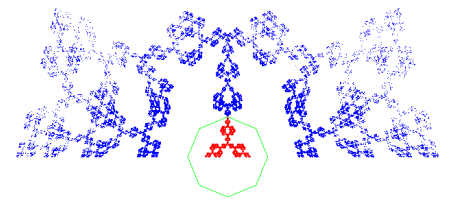


Figure 6(b)

The Boundary of Koch snowflake and its image under $I_{\frac{\pi}{4}}(O, r)$ The Koch anti snowflake and its image under $I_{\frac{\pi}{4}}(O, r)$

4. Alpha Circle Inversion Fractal

In this section, we study α -circle inversion fractals, and generalize the circle inversion fractals method which is introduced by Frame and Cogevina [9] with using α -circle inversion.

Let C_1, C_2, \dots, C_n be distinct n alpha circles and $I_\alpha(O_1, r_1), I_\alpha(O_2, r_2), \dots, I_\alpha(O_n, r_n)$ be α -circle inversion with respect to C_1, C_2, \dots, C_n , respectively. Let \mathcal{G} be collection of all combinations of the α -circle inversions. For any point X external to all the C_i , $\mathcal{G}(X) = \{I_\alpha(O, r)(X) : I_\alpha(O, r) \in \mathcal{G}\}$ is called the orbit of X . The set of accumulation points of the orbit of X under \mathcal{G} is termed as the limit set and denoted by $\Lambda(C_1, \dots, C_n)$. There are the limit sets of alpha circle inversions such as the fractals generated by iterated function systems (IFS), and they are often fractal. An Iterated Alpha Circle Inversion System (IACIS) is a finite collection $\{I_\alpha(O_1, r_1), I_\alpha(O_2, r_2), \dots, I_\alpha(O_n, r_n)\}$ of alpha circle inversion mappings. But an IACIS is not an IFS. According to the definition of IFS, IFSs require a complete metric space and a finite set of contraction mappings which are defined on complete metric space. But α -circle inversion mappings are not contraction mappings for all sets within $\mathbb{R}_\alpha^2 \cup \{P_\infty\}$. Case (iv) of Proposition 2 states that the α -circle inversions are only contraction mappings for exterior to the circle of inversion. Then it is necessary to make restriction on the initial placement of the inversion circles and also domain of inversion mappings in order to be able to use IACIS such as IFS. In this case there are two situations according to the initial circle placement. These situations are non-overlapping circle placement and overlapping circle placement. In non-overlapping circle placement, circles have disjoint

interior but they can have common point(s) on their boundaries. We will start with the non-overlapping circle case. If the initial circle placement is totally disjoint, then the resulting limit set is wholly contained within $\bigcup_{i=1}^N C_i$. Throughout the iteration process all point are inverted by using contractive inversion mappings. This process results in a nested sets of inversion image closed curve being formed. The length of radii of these image closed curve decrease throughout the iteration process covering to zero, forming a collection of limit points. The union of these limit points is named the limit set of IACIS.

Now we consider the overlapping circle case. If the interiors of the circles of inversion overlap we can not assume convergence to a limit set. Once a point is contained with a circle of inversion, all subsequent inversion must lie within or on the boundary of an initial circle of inversion under IACIS for non-overlapping circle. If circles of inversion overlap, then it is possible for a point within a circle of inversion, more specifically in the section of overlap, to be inverted outside all circles of inversion. To get over this problem, the concept of restricted limit set was introduced by Clancy and Frame [7]. The restricted limit set is defined as follows: "Limit set of the orbit of a point, with the restriction that if some orbit point P_i lies in the disc bounded by C_j , then the next orbit point P_{i+1} , cannot be in $I_\alpha(O_j, r_j)(P_j)$ ". If the circle placement has disjoint interiors the above restriction reduces to "never inverting in the same circle twice".

Now in order to visualize the limit set of IACIS we give an algorithm which is modified version of the random inversion algorithm introducing by Frame and Cogevina [9]. The modification is only Euclidean circle inversion replaced by α -circle inversion.

Algorithm 1 Random α -circle inversion algorithm

Input: The set of α -circle $\{C_1, C_2, \dots, C_n\}$ of inversion. P_0 is starting point external to all the C_i .

$n > 20$ number of iterations.

Output: Approximation of a restricted limit set (α -circle inversion fractal)

- 1) $j = \text{random number from } \{1, \dots, n\}$
 - 2) $P = I_\alpha(O_j, r_j)(P_0)$
 - 3) **for** i **from** 2 **to** n **do**
 - 4) $l = \text{random number from } \{1, \dots, n\}$
 - 5) **while** $j = l$ **or** $P \in \text{int}(C_l)$ **do**
 - 6) $l = \text{random number from } \{1, \dots, n\}$
 - 7) **end while**
 - 8) $j = l$
 - 9) $P = I_\alpha(O_j, r_j)(P)$
 - 10) **if** $i > 20$ **then**
 - 11) Plot P
 - 12) **end if**
 - 13) **end for**
-

A set of α -circle inversion mappings, a starting point that lies outside of all the α -circles and the number of iterations are required to visualize and produce the approximation of the restricted limit set.

First, starting point which lies outside of all the C_i is mapped to the point which lies in any α -circles C_i by using randomly choosing α -circle inversion. Then for each new iteration an α -circle inversion is randomly chosen with two restrictions. Since the inversion is an involution, the first restriction is that any mapping be not used consecutively. The second restriction is that the point which is obtained the previous iteration must not be inside the α -circle which is randomly chosen inversion mapping. Because we want to the inversion mappings to be a contraction not an expansion. Moreover, the contraction guarantees the convergence of the algorithm.

The α -circle inversion fractals which are shown in Figures 7-12 are obtained by using Algorithm 1.

Example 4.1. Figure 7 illustrate one each example two different cases about limit set of some α -circles according to placements of these circles. Each of these example shows that the limit set of four α -circles such that $\alpha = \pi/4$. Looking at the leftmost figure, four circles positioned tangentially to each other and their limit set is seen. Note that since all circles are connected, there is no gap in the limit set which is obtained using

these circles. That is, limit set would be a Cantor set wrapped around limit set in the case which is not include gap. In the middle figure, four circles positioned so that they have no common point with each other and their limit set is seen. Therefore since all possible intersections of these circles is empty, limit set of corresponding to this situation would be gaps. If the small black rectangle on the middle figure in Figure 7 is magnified, then as shown in rightmost figure in Figure 7, in the limit set of these situation has been gaps like as Cantor set.

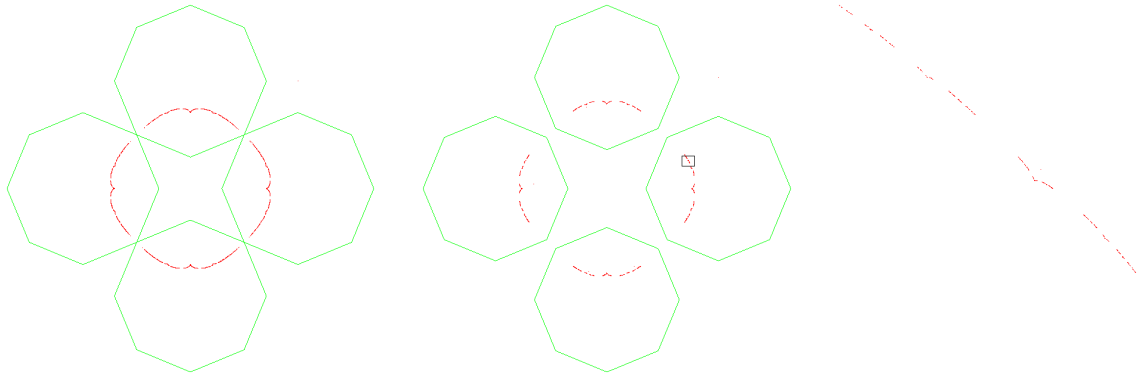


Figure 7

α -circle inversion fractal for touching α -circles and non-touching α -circles

Example 4.2. Figure 8 and Figure 9 illustrate some examples of the limit set of non-overlapping but tangent α -circles with different initial circle placement of which their produced by using Algorithm 1. In each cases of Figure 8, there are five non-overlapping and tangent alpha circles as initial circle placements. In the first two figures of Figure 8, when the α -circles have same type but different radii, in the last figure of Figure 8 the α -circles have different type and radii. Similarly in each cases of Figure 9, there are nine non-overlapping and tangent α -circles as initial circle placements. First, second and third figure of Figure 9 have one type, two different type and three different type α -circles, respectively.

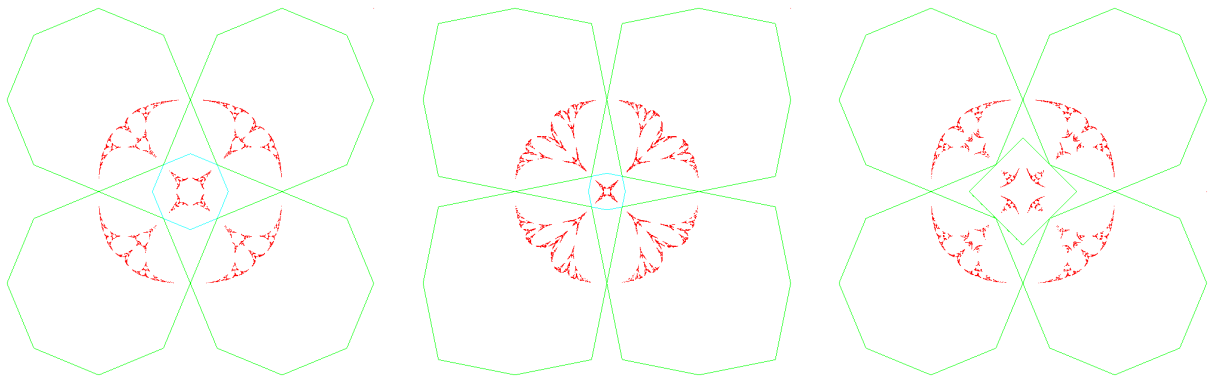


Figure 8

Three example of α -circle inversion fractal of five non-overlapping and tangent α -circles

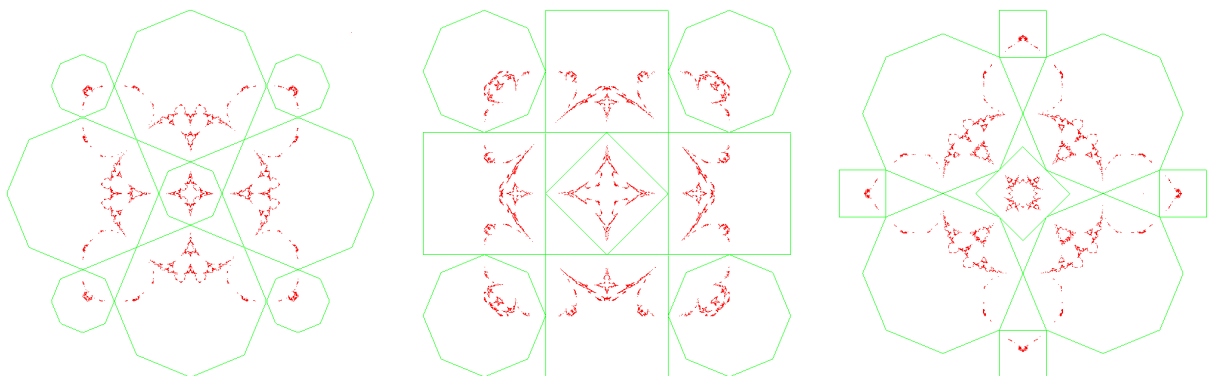


Figure 9

Three example of α -circle inversion fractal of nine non-overlapping and tangent α -circles

Example 4.3. Each figure in Figure 10 has four red α -circles of the same or different type, none of which are inside the other, positioned only externally tangentially. Let first of all each α -circle invert according to the other α -circles except itself. Later we invert again obtained images according to α -circles. At this stage, we invert only to the obtained images that are outside the inversion α -circle. This process is then repeated indefinitely. Ultimately, the limit set is reached at infinity. This process also explains whether consist of gaps or not which is highlighted in Example 4.1. In Figure 10, we see the first four stages of this process for three different situations.

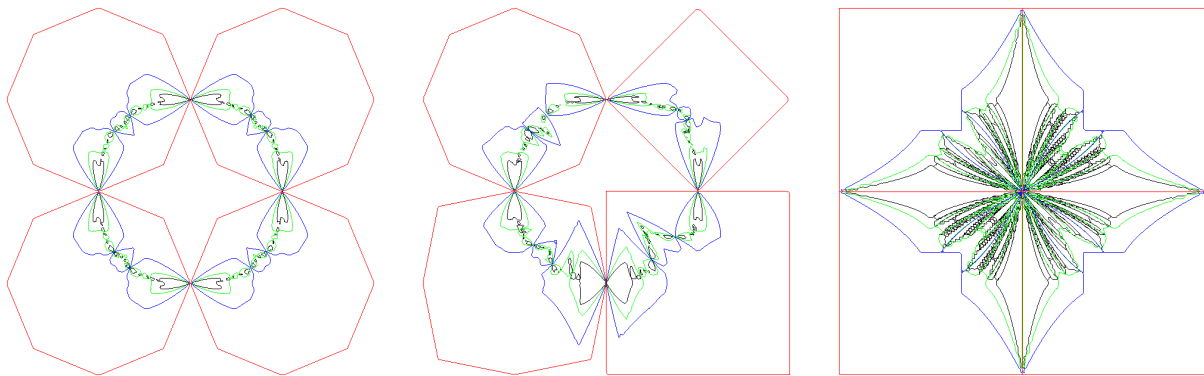


Figure 10

The process inverting all each α -circle and their images according to the other α -circles except itself.

Example 4.4. Figure 11 and Figure 12 illustrate some examples of the limit set of overlapping α -circles with different initial circle placement of which their produced by using Algorithm 1. In each cases of Figure 11, there are five overlapping α -circles such that two different types as initial circle placements. Similarly in each cases of Figure 12, there are eight or nine overlapping α -circles such that two or three different types as initial circle placements. While mostleft and most right figure of Figure 12 have nine α -circles with three different types, the middle figure of the Figure 12 have eight α -circles with two different types.

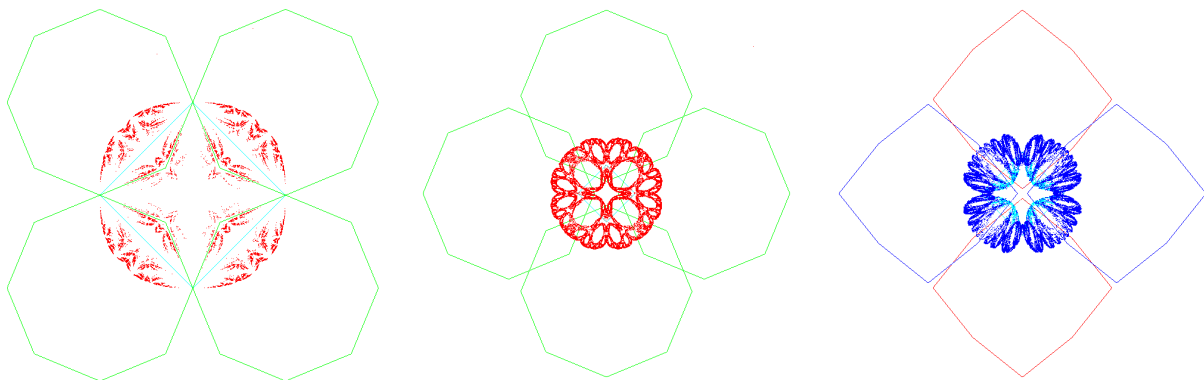


Figure 11

Three example of α -circle inversion fractal of five overlapping α -circle

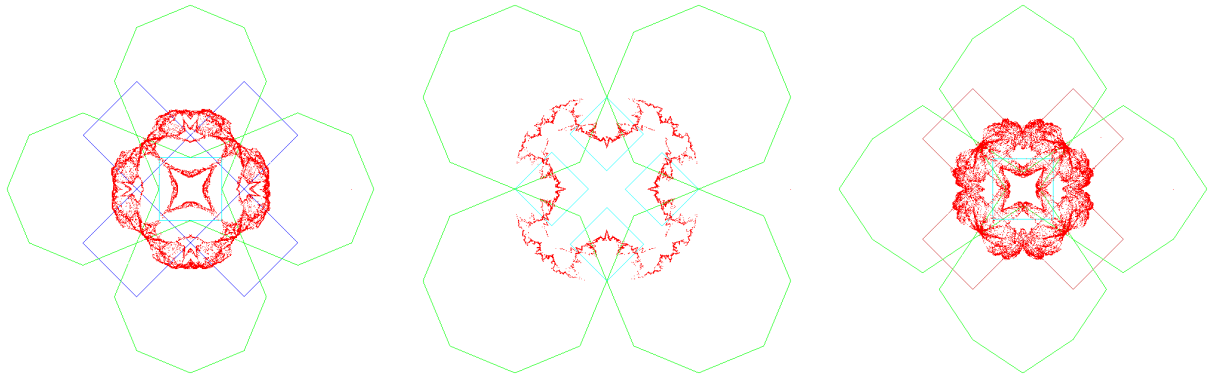


Figure 12

Three example of α -circle inversion fractal of eight or nine overlapping α -circle

5. Fractal Patterns By Using Star-Shaped Set Inversion

In [11] Gdawiec states that since circles are star-shaped sets, circle inversion is the special case of star-shaped set inversion. In other words, star-shaped set inversion is an expansion of circle inversion. Now we give some required definitions and properties from [11].

Definition 5.1. A set $S \subset \mathbb{R}^2$ is star-shaped if there exists a point $P \in \text{int}(S)$ such that for all points $F \in S$ the line segment \overline{PF} lies entirely within S . The locus of the points P having the above property is the kernel of S .

Definition 5.2. Let S be a star-shaped set and $Q=(a, b)$ be a point belongs to the kernel of S . The star-shaped set inversion with respect to S is the mapping $\phi_S: \mathbb{R}^2 \setminus \{Q\} \rightarrow \mathbb{R}^2 \setminus \{Q\}$ defined by $\phi_S(P) = P'$, where P' lies on the ray \overrightarrow{QP} and $d(Q, P)d(Q, P') = d(Q, T)^2$, where T is the intersection of the ray \overrightarrow{QP} with the boundary of S .

Let S be a star-shaped set and let $Q = (a, b)$ be a point that belongs to the kernel of S . Then the star-shaped set inversion of the point $P = (x, y)$ with respect to S is the point

$$x' = a + \frac{d(Q, T)^2 (x - a)}{(|x - a|^2 + |y - b|^2)},$$

$$y' = b + \frac{d(Q, T)^2 (y - b)}{(|x - a|^2 + |y - b|^2)},$$

where T is the intersection of the ray \overrightarrow{QP} with the boundary of S .

Now, we define alpha star-shaped set inversion.

Definition 5.3. Let S be an star-shaped set and point Q belongs to kernel of S . Also P_∞ denote the ideal point adjoining one to the alpha plane. In \mathbb{R}_α^2 the alpha star-shaped set inversion with respect to Q is the function such that

$$I_\alpha(Q) : \mathbb{R}_\alpha^2 \cup \{P_\infty\} \rightarrow \mathbb{R}_\alpha^2 \cup \{P_\infty\}$$

defined by $I_\alpha(Q)(Q) = P_\infty$, $I_\alpha(Q)(P_\infty) = Q$ and $I_\alpha(Q)(P) = P'$ for $P \neq Q, P_\infty$ where P' is on the ray \overrightarrow{QP} , point T is intersection point \overrightarrow{QP} and S , and $d_\alpha(Q, P)d_\alpha(Q, P') = [d_\alpha(Q, T)]^2$. The point P' is called the alpha star-shaped set inverse of P in S , Q is called the center of inversion.

Note that we obtain the alpha star-shaped set inversion replacing Euclidean distance in definition of star-shaped set inversion by an α -distance. Therefore we get the following generalization of star-shaped set inversion.

Theorem 5.1. Let S be a star-shaped set and let $Q = (a, b)$ be a point that belongs to the kernel of S . Then the alpha star-shaped set inversion of the point $P = (x, y)$ with respect to S is the point

$$x' = a + \frac{d_\alpha(Q, T)^2 (x - a)}{(\max\{|x - a|, |y - b|\} + \lambda(\alpha) \min\{|x - a|, |y - b|\})^2},$$

$$y' = b + \frac{d_\alpha(Q, T)^2 (y - b)}{(\max\{|x - a|, |y - b|\} + \lambda(\alpha) \min\{|x - a|, |y - b|\})^2},$$

where T is the intersection of the ray \overrightarrow{QP} with the boundary of S .

Now in order to visualize the limit set of alpha star-shaped set inversions we give an algorithm which is modified version of the random inversion algorithm introduced by Gdawiec [11]. The modification relies on the replacement of the Euclidean star-shaped set inversion by the alpha star-shaped set inversion.

Algorithm 2 Random alpha star-shaped set inversion algorithm

Input: The set of α -star-shaped sets $\{S_1, S_2, \dots, S_n\}$

with chosen centers of inversion.

P_0 is starting point external to all the S_i .

$n > 20$ number of iterations.

Output: Approximation of a restricted limit set (alpha star-shaped sets inversion fractal)

1) j = random number from $\{1, \dots, n\}$

2) $P = I_\alpha(Q_j)(P_0)$

3) **for** i **from** 2 **to** n **do**

4) l = random number from $\{1, \dots, n\}$

5) **while** $j = l$ **or** $P \in \text{int}(S_i)$ **do**

6) l = random number from $\{1, \dots, n\}$

7) **end while**

8) $j = l$

9) $P = I_\alpha(Q_j)(P)$

10) **if** $i > 20$ **then**

11) Plot P

12) **end if**

13) **end for**

A set of alpha star-shaped set inversion mappings, a starting point that lies outside of all the star-shaped sets and the number of iterations are required to visualize and produce the approximation of the fractal set.

First, starting point which lies outside of all the S_i is mapped to the point which lies in any star-shaped sets S_i by using randomly choosing alpha star-shaped set inversion. Then for each new iteration a alpha star-shaped set inversion is randomly chosen with two restrictions. Since the alpha star-shaped set inversion is an involution, the first restriction is that any mapping be not used consecutively. The second restriction is that the point which is obtained the previous iteration must not be inside the star-shaped set which is randomly chosen alpha star-shaped set inversion mapping. Because we want to the inversion mappings to be a contraction not an expansion. Moreover, the contraction guarantees the convergence of the algorithm.

Example 5.1. Figure 13, Figure 14 and Figure 15 illustrate some examples of the alpha star-shaped set inversion fractals obtained by applying Algorithm 2. Each of three figures in Figure 13 there are the same initial alpha star-shaped sets placement which have nine overlapping α -circles with two different types. While every figures of the Figure 13 have the same initial alpha star-shaped sets placement, every shapes of in all cases of the Figure 13 have different inversion centers which is shown marked as black point. Thus, although the initial alpha star-shaped sets placement is the same, it can be observed how the alpha star-shaped set inversion fractals changed as the inversion centers changed.

Similarly, each of three figures in Figure 14 there are the same initial alpha star-shaped sets placement which have eight overlapping the same type α -circles with two different radii. But in every cases of the Figure 14 every shapes have different inversion centers which is shown marked as black point. So just as the Figure 13, the Figure 14 give chance for observing how the alpha star-shaped set inversion fractals changed as the inversion centers changed.

In Figure 15 like as Figure 13 and Figure 14 there are the same initial alpha star-shaped sets placement which have nine overlapping α -circles with three different types. But in every cases of the Figure 15 every shapes have different inversion centers which is shown marked as black point. So just as the Figure 14 and the Figure 14, the Figure 15 give chance for observing how the alpha star-shaped set inversion fractals changed as the inversion centers changed. The alpha star-shaped set inversion fractals obtained by applying Algorithm 2 is red points showing like dust cloud in Figure 13, 14, 15.

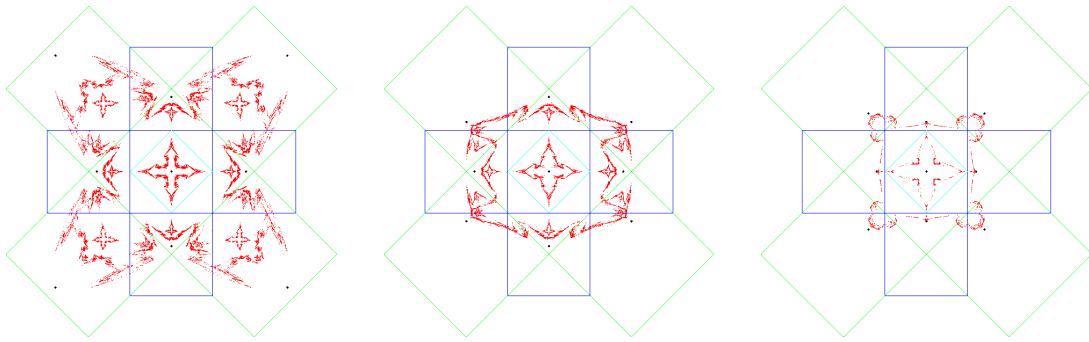


Figure 13

The variation of alpha star-shaped set inversion fractals according to the position of the inversion centers

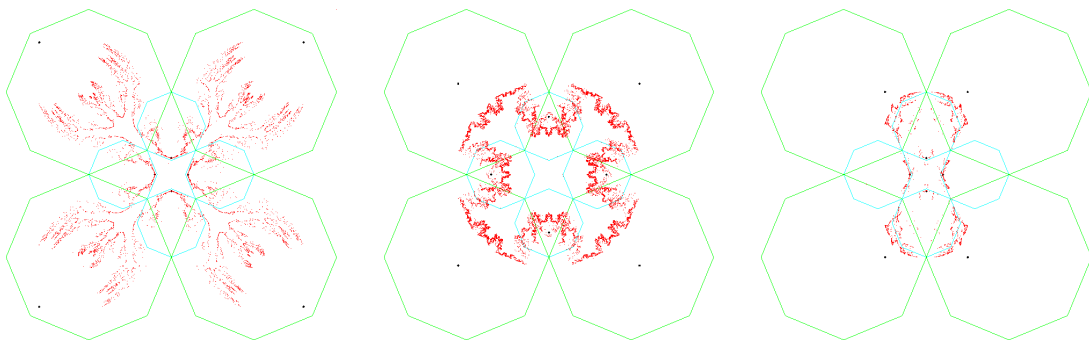


Figure 14

The variation of alpha star-shaped set inversion fractals according to the position of the inversion centers

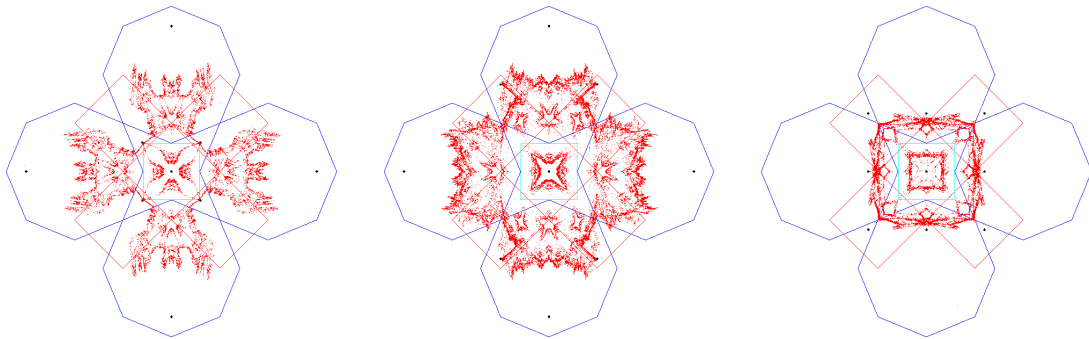


Figure 15

The variation of alpha star-shaped set inversion fractals according to the position of the inversion centers

6. Conclusions

In this paper we defined the α -circle inversion by replacing Euclidean metric with α -metric. Later, we presented modification of circle inversion fractals. The proposed modification was based on the use of α -circle inversion in the circle inversion methods. Moreover, in alpha plane, \mathbb{R}_α^2 , we gave a generalization of α -circle inversion fractal by using the concept of star-shaped set inversion which is a generalization of circle inversion fractal. The patterns obtained with the proposed modifications is notably different from the original ones, and they form new fractal shapes. Obtained interesting and aesthetic new fractals can be used as textiles, wallpapers, or ceramic patterns.

Acknowledgements

We would like to thank the referees and editor for reviewing the paper carefully and their valuable comments to improve the quality of the paper.

Availability of data and materials

Not applicable.

Competing interests

The authors declare that they have no competing interests.

Author's contributions

All authors contributed equally to the writing of this paper. All authors read and approved the final manuscript.

References

- [1] Barnsley, M.: *Fractals Everywhere*. Academic Press, Boston (1988).
- [2] Bayar, A., Ekmekci, S.: *On circular inversions in taxicab plane*. J. Adv. Res. Pure Math. **6** (4), 33-39 (2014).
- [3] Blair, D.: *Inversion Theory and Conformal Mapping*. Student Mathematical Library, American Mathematical Society, 9 (2000).
- [4] Boreland, B., Kunze, H.: *Circle Inversion Fractals*. In: Belair, J., Frigaard, L., Kunze, H., Makarov, R., Melnik, R., Spiteri, R. (eds) *Mathematical and Computational Approaches in Advancing Modern Science and Engineering*, Springer, Cham. 609-619 (2016).
- [5] Brown, C. T., Witschey, W. R. T. and Liebovitch, L. S.: *The Broken past: Fractals in Archaeology*. Journal of Archaeological Method and Theory. **12** (1), 37-78 (2005).
- [6] Childress, N.: *Inversion with respect to the central conics*. Mathematics Magazine. **38** (3), 147-149 (1965).
- [7] Clancy, C. and Frame M.: *Fractal geometry of restricted sets of circle inversions*. Fractals. **3** (4), 689-699 (1995).
- [8] Colakoglu, H. B.: *Concerning the alpha distance*. Algebras Groups Geom. **8**, 1-14 (2011).
- [9] Frame, M., Cogevina, T.: *An infinite circle inversion limit set fractal*. Comput. Graph. **24**(5), 797-804 (2000).
- [10] Fitzsimmons, M., Kunze, H.: *Circle Inversion IFS*. Springer Proceedings in Mathematics & Statistics. **259**, 81-91 (2018).
- [11] Gdawiec, K.: *Star-shaped set inversion fractals*. Fractals. **22** (4), 1450009-1-1450009-7 (2014).
- [12] Gdawiec, K.: *Pseudoinversion Fractals*. Lecture Notes in Computer Science. **9972**, 29-36 (2016).
- [13] Gdawiec, K.: *Inversion Fractals and Iteration Processes in the Generation of Aesthetic Patterns*. Computer Graphics Forum. **36** (1), 35-45 (2017).
- [14] Gelişgen, O., & Kaya, R.: *On α_i -distance in Three Dimensional Space*. Applied Sciences (APPS). **8**, 65-69 (2006).
- [15] Gelişgen, O., & Kaya, R.: *Generalization of α -distance to ndimensional Space*. Scientific-Professional Information Journal of Croatian Society for Constructive Geometry and Computer Graphics (KoG). **10**, 33-35 (2006).
- [16] Helt, G.: *Inversive Diversions and Diverse Inversions*. Bridges Conference Proceedings, 467-470 (2017).
- [17] Kozai, K., Libeskind, S.: *Circle Inversions and Applications to Euclidean Geometry*. online supplement to Euclidean and Transformational Geometry: A Deductive Inquiry.
- [18] Leys, J.: *Sphere inversion fractals*. Comput. Graph. **29** (3), 463-466 (2005).
- [19] Losa, G. A., Merlini, D., Nonnenmacher, T. F., Weibel E. R.: *Fractals in Biology and Medicine*. Birkhäuser Basel (1998).
- [20] Mandelbrot, B.: *The Fractal Geometry of Nature*. W. H. Freeman and Company, New York (1983).
- [21] Nickel, J. A.: *A Budget of inversion*. Math. Comput. Modelling. **21** (6), 87-93 (1995).
- [22] Ostwald, M.J.: *Fractal Architecture: Late Twentieth Century Connections Between Architecture and Fractal Geometry*. Nexus Netw J. **3**, 73-84 (2001).
- [23] Patterson, B. C.: *The origins of the geometric principle of inversion*. Isis. **19** (1), 154-180 (1933).
- [24] Ramirez, J. L.: *Inversions in an Ellipse*. Forum Geometricorum. **14**, 107-115 (2014).
- [25] Ramirez, J. L. G., Rubiano N. & Zlobec, B. J.: *Generating Fractal Patterns by Using p -Circle Inversion*. Fractals. **23** (4), 1550047-1-1550047-13 (2015).
- [26] Smith, R.: *Fractal producing iterative mapping systems on circles*. M.S. thesis, University of Newcastle, Australia (2010).
- [27] Tian, S.: *Alpha Distance-A Generalization of Chinese Checker Distance and Taxicab Distance*. Missouri J. of Math. Sci. (MJMS). **17** (1), 35-40 (2005).
- [28] Zhang, Y., He, X.: *Fractal geometry derived from geometric inversion*. Comput. Graph. **11** (11), 1075-1079 (1990).

Affiliations

ÖZCAN GELİŞGEN

ADDRESS: Eskişehir Osmangazi University, Department of Mathematics and Computer Sciences, 26040, Eskişehir-TURKEY.

E-MAIL: gelisgen@ogu.edu.tr

ORCID ID:0000-0001-7071-6758

TEMEL ERMİŞ

ADDRESS: Eskişehir Osmangazi University, Department of Mathematics and Computer Sciences, 26040, Eskişehir-TURKEY.

E-MAIL: termis@ogu.edu.tr

ORCID ID:0000-0003-4430-5271